

## SYNTHESIS AND ELECTROCHEMICAL PERFORMANCE OF ULTRATHIN WS<sub>2</sub> NANOSHEETS

X. H. ZHANG<sup>a\*</sup>, H. TAN<sup>a</sup>, Z. FAN<sup>a</sup>, M. Z. GE<sup>b</sup>, X. YE<sup>a</sup>, M. Q. XUE<sup>c</sup>

<sup>a</sup>*School of Mechanical Engineering, Jiangsu University of Technology, Changzhou 213001, Jiangsu Province, China*

<sup>b</sup>*School of Materials and Engineering, Jiangsu University of Technology, Changzhou 213001, Jiangsu Province, China*

<sup>c</sup>*Changzhou Vocational Institute of Light Industry, Changzhou, 213164, Jiangsu Province, China*

In this work, ultrathin WS<sub>2</sub> nanosheets were synthesized through a facile solid-state reaction route. The as-synthesized samples were characterized by X-ray diffraction (XRD), scanning electron microscopy (SEM) and transmission electron microscopy (TEM). The electrochemical performance of ultrathin WS<sub>2</sub> nanosheets as anode material for lithium-ion batteries were systematically investigated by a variety of electrochemical testing techniques. It was found that WS<sub>2</sub> nanosheets exhibited a relatively high reversible capacity and fine cycle performance.

(Received July 22, 2017; Accepted October 2, 2017)

*Keywords:* WS<sub>2</sub>; nanosheets; lithium-ion batteries; cycle performance

### 1. Introduction

Li-ion batteries (LIBs), as one kind of energy storage devices, have been the dominant power source for various portable electronic devices in modern society. But their energy and power densities, cycle life and rate capability have to be improved to meet the more demanding specifications of power-intensive applications such as the electric vehicles [1-3]. The performance of LIBs is largely dependent on the electrode materials. Currently, graphite has been widely used as the anode material in the commercial LIBs due to its natural abundance and stable cycling performance. However, the relatively low theoretical capacity (372 mAh g<sup>-1</sup>) and poor rate-capability of graphite makes it important to find alternative anode materials [4-6].

Recently, ultrathin 2D nanomaterials have attracted much attention because of their unique electronic and physical properties [7-9]. These 2D nanosheets are now considered to be the excellent candidates as the electrode materials for LIBs due to their shorter path length and more channels for lithium ion diffusion [10, 11]. Among these 2D nanosheets, graphene has been the most extensively studied and the enhanced lithium storage capacity of graphene in lithium ion cells has been experimentally verified [10, 12]. Other 2D nanosheets have also emerged such as transition-metal dichalcogenides (TMDs), whose unique electrical and optical properties are of interest to transistors, [13] phototransistors, [14] sensitive sensors [15] and lithium ion battery anodes. [16] WS<sub>2</sub>, as one member of this family, also is an alternative anode material for lithium-ion batteries. Over the past few decades, WS<sub>2</sub> nanoparticles with various morphologies and sizes have been synthesized and they have demonstrated a stable cyclability [17-21]. However, the electrochemical performance of ultrathin WS<sub>2</sub> nanosheets has rarely been investigated.

Until now, many approaches have been used to prepare ultrathin WS<sub>2</sub> nanosheets, and the top-down and bottom-up strategies are two major synthesis routes. The top-down methods rely on

---

\*Corresponding author: zxhstu@yahoo.com

the exfoliation of layered bulk crystals, which include the mechanical cleavage and chemical exfoliation [22-25]. However, these approaches are frequently deficient in the yield and the manufacturing processes of these approaches are complicated. Recently, the bottom-up approaches have been used to synthesize few-layered WS<sub>2</sub> nanosheets. For example, Yang [26] and Ratha et al. [27] synthesized the ultrathin WS<sub>2</sub> nanosheets by an one-pot hydrothermal reaction of WCl<sub>6</sub> and thioacetamide at 265 °C for 24 h. But, it still remains a major challenge to develop simple, reproducible and economical synthetic approach for the fabrication of ultrathin WS<sub>2</sub> nanosheets.

In this study, the ultrathin WS<sub>2</sub> nanosheets were prepared by a facile solid phase reaction method using WO<sub>3</sub> and thiourea as the starting materials. The electrochemical performance of WS<sub>2</sub> nanosheets were investigated by a variety of electrochemical testing techniques.

## 2. Experimental

### 2.1 Synthesis of Ultrathin WS<sub>2</sub> Nanosheets

The raw materials, thiourea and tungsten trioxide (WO<sub>3</sub>), were purchased from Aladdin Chemical Reagent Company and used as received. The reaction was carried out in a tube furnace. In the typical synthesis, 10 g of thiourea and 0.5g of WO<sub>3</sub> were thoroughly ground with mortar and pestle for 30 min, and then the mixture was transferred in a corundum boat. Prior to the synthesis, the tube furnace was raised temperature at a rate of 10 °C/min under nitrogen. When the temperature reached 850 °C, the corundum boat was quickly pushed into the hot zone of the tube furnace and heated at 850 °C for 1 h. After the heating step, the temperature was decreased to room temperature and the product was collected.

### 2.2 Characterization of Ultrathin WS<sub>2</sub> Nanosheets

The X-ray diffraction (XRD) patterns were recorded using Japan Shimadzu LabX XRD-6000 X-ray diffractometer with Cu K $\alpha$  radiation ( $\lambda = 0.1546$  nm). The  $2\theta$  range used in the measurement was from 10° to 80° with a velocity of 5° /min. The morphologies of the as-synthesized products were examined by field-emission scanning electron microscopy (FESEM, JEOL, JSM-7001F) and transmission electron microscopy (TEM, JEOL, JEM-2100).

### 2.3 Electrochemical measurement

The electrochemical measurements were performed using two-electrode test cells. The working electrodes were fabricated by following slurry coating processing: First, 80 wt% active material, 10 wt% conductivity agent (Super P carbon black) and 10 wt% binder (polyvinylidene fluoride) were mixed; then the mixed slurry was coated on a pure Cu foil; at last, the coated Cu foil was dried at 120°C for 12 h in vacuum and compressed. The test cells was assembled in an argon-filled glovebox, using a lithium sheet as the counter and reference electrode, a polypropylene film (Celgard 2400) separator, and an electrolyte of 1.0 M LiPF<sub>6</sub> solution in a 1:1 (v/v) mixture of ethylene carbonate and dimethyl carbonate. The charge/discharge measurements were performed using a NEWWARE battery tester between 0.01~ 3 V at the current density of 100 mA g<sup>-1</sup>.

## 3. Results and discussion

### 3.1 Structural and Morphological Characterization of Ultrathin WS<sub>2</sub> Nanosheets

The crystalline structure and phase composition of the synthesized samples were confirmed by powder X-ray diffraction. A typical XRD pattern of the obtained ultrathin WS<sub>2</sub> nanosheets is shown in Fig. 1a. The peaks at  $2\theta = 14.12^\circ, 28.42^\circ, 32.72^\circ, 39.32^\circ, 59.24^\circ,$  and  $69.54^\circ$  were correlated to the (002), (004), (100), (103), (008), and (108) planes of WS<sub>2</sub>, respectively, and all the diffraction peaks can be indexed to hexagonal phase of WS<sub>2</sub> (JCPDS Card No. 08-0237). No peaks of other impurity phases are detected from this pattern. EDS spectrum is presented in Fig.

1b, which reveals that the sample consisted of element W and S, no other element is observed. Moreover, the quantification of the peaks shows that the molar ratio of W to S is about 1:1.95, which is almost consistent with the stoichiometric  $WS_2$ .

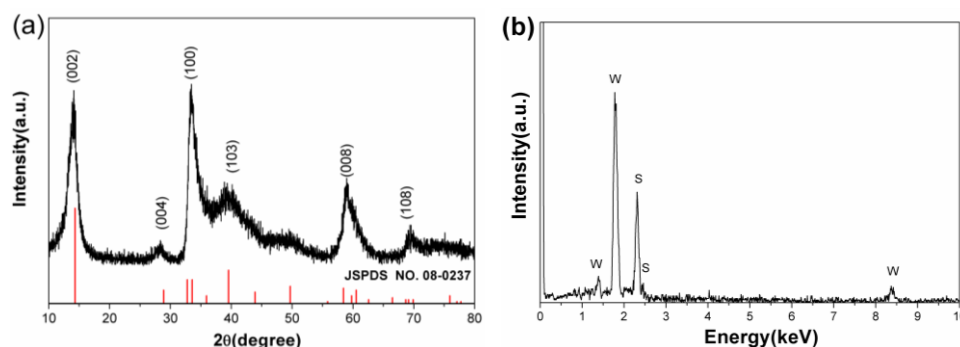


Fig. 1 (a) XRD pattern and (b) EDS of the as-prepared  $WS_2$  nanosheets

The morphology and size of  $WS_2$  samples were identified by SEM and TEM. The low magnification SEM image shown in Fig. 2a clearly reveals that the obtained samples consist of a large number of ultrathin sheets. To further expose the microstructure of these sheets, the high-magnification SEM image (Fig. 2b) is also observed. It shows that the prepared nanosheets are stacked loosely, and the width of the nanosheets is in the range of 200-300 nm, the thickness of the nanosheets is  $\sim 10$  nm. Fig. 2c and 2d are the TEM images of  $WS_2$  nanosheets. The low magnification TEM image (Fig. 2c) demonstrates that the samples are composed of graphene-like nanosheets with lateral size of 300-500 nm. In addition, it is also observed that a fraction of  $WS_2$  nanosheets are curved. The main stimulus for the curve of sheets would be elimination of dangling bonds at the edges [28]. In Fig. 2c, the uniform few-layer  $WS_2$  sheets are observed, implying that the  $WS_2$  exhibits a high crystallinity and good uniformity. The edge structure of the as-grown  $WS_2$  sheets is shown by the high magnification TEM image in Fig. 2d. The interlayer separation between the  $WS_2$  layers is 0.65 nm, and is slightly larger than the interplanar distance for the (002) plane of the bulk  $WS_2$ .

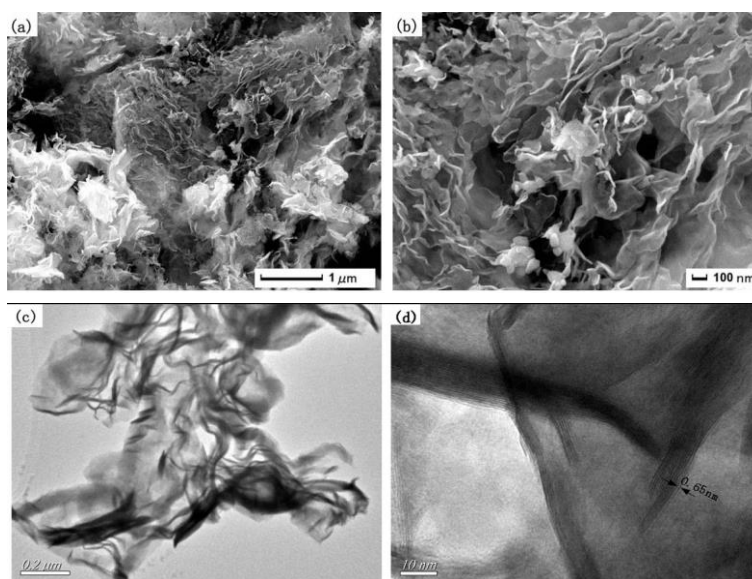


Fig. 2. FESEM (a,b) and TEM (c,d) images of the  $WS_2$  nanosheets obtained at 850 °C for 1 h

### 3.2 Electrochemical Performance

Electrochemical measurement was performed to evaluate the electrochemical lithiation/delithiation performances of ultrathin WS<sub>2</sub> nanosheets as the cathode materials of LIBs. Fig. 3a shows the first three charge and discharge voltage curves of the ultrathin WS<sub>2</sub> nanosheets measured at a current density of 100 mA g<sup>-1</sup> and voltage range of 0.01-3V. In the first discharge process, two clear voltage plateaus at about 1.0 and 0.75 V were observed. The plateau at 1.0 V is attributed to the intercalation of Li<sup>+</sup> into WS<sub>2</sub> lattice to form Li<sub>x</sub>WS<sub>2</sub>, changing the WS<sub>2</sub> structure from 2H (trigonal prismatic) to 1T (octahedral) [18, 19]. The plateau at 0.75 V is due to the conversion reaction in which Li<sub>x</sub>WS<sub>2</sub> is decomposed into W particles and Li<sub>2</sub>S [19, 20]. The overall reaction during this process can be described as: WS<sub>2</sub> + xLi<sup>+</sup> + xe<sup>-</sup> = Li<sub>x</sub>WS<sub>2</sub>, Li<sub>x</sub>WS<sub>2</sub> + (4 - x)Li → W + 2Li<sub>2</sub>S. [21] Voltage profiles during the 2<sup>nd</sup> and 3<sup>rd</sup> discharge processes are clearly different from those of the 1<sup>st</sup> cycle. Two potential plateaus at 2.2 V and 1.7 V are observed, which might correspond to the lithiation of S and insertion of Li<sup>+</sup>, respectively. In the charging process, a plateau at about 2.2 V can be clearly identified for the first and subsequent cycles, corresponding to the oxidation of Li<sub>2</sub>S. [17,18]

The cycling performance and their Coulombic efficiencies of the WS<sub>2</sub> electrodes are shown in Fig. 3(b). The initial discharge and charge capacities were 755 and 630 mA h g<sup>-1</sup>, respectively. The Coulombic efficiency is 83.4% and the irreversible capacity of 125 mA h g<sup>-1</sup> in the first cycle may be caused by the decomposition of the electrolyte and formation of the solid electrolyte interface, which is common in transition metal sulfide anodes. The Coulombic efficiency was greatly enhanced after the formation cycle, achieving 95.9% and 94.1% during the 2<sup>nd</sup> and 3<sup>rd</sup> cycles, with charge capacities of 605 and 594 mA h g<sup>-1</sup>, respectively. In addition, the reversible capacity remains 553–640 mA h g<sup>-1</sup>, with a capacity retention of 86.4% during the following 50 cycles (Fig. 4b), indicating that the ultrathin WS<sub>2</sub> nanosheets have excellent cycling performance.

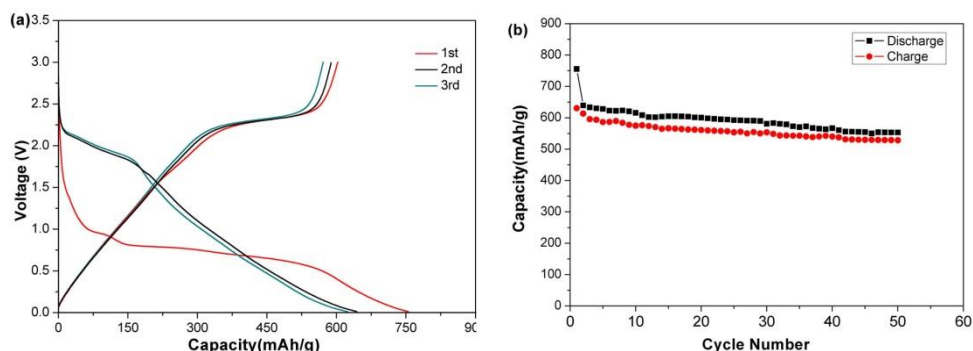


Fig. 3 (a) The first three charge/discharge voltage profiles and (b) the cycling performance of ultrathin WS<sub>2</sub> nanosheets at a current density of 100 mA g<sup>-1</sup>.

## 4. Conclusion

In summary, ultrathin WS<sub>2</sub> nanosheets with thickness of ~10 nm were successfully prepared by a solid phase reaction. The ultrathin WS<sub>2</sub> nanosheets showed superior electrochemical performance in many cycles: the charge–discharge capacities of 553 mA h g<sup>-1</sup> still maintained after 100 cycles at a current density of 100 mA g<sup>-1</sup>. This work provided a facile way to form other structures anode materials for LIBs and promised for developing a better performing rechargeable energy storage system that is both cost effective and environmentally friendly.

## Acknowledgements

This work was financially supported by the Changzhou Sci&Tech Program (CJ20159048), the Natural Science Foundation of the Jiangsu Higher Education Institutions of China (14KJB460012, 16KJB430031), and the research fund of Jiangsu Province Cultivation base for State Key Laboratory of Photovoltaic Science and Technology (SKLPSTKF201508).

## References

- [1] D.A.C. Brownson, D.K. Kampouris, C.E. Banks, *J. Power Sources* **196**, 4873 (2011).
- [2] G. X. Wang, X.P. Shen, J. Yao, J. Park, *Carbon* **47**, 2049 (2009).
- [3] E. Yoo, J. Kim, E. Hosono, H. Zhou, T. Kudo, I. Honma, *Nano Lett.* **8**, 2277 (2008).
- [4] K. Sato, M. Noguchi, A. Demachi, N. Oki, M. Endo, *Science* **264**, 556 (1994).
- [5] M.S. Whittingham, *Chem. Rev.* **104**, 4271 (2004).
- [6] F.Y. Cheng, Z.L. Tao, J. Liang, J. Chen, *Chem. Mater.* **20**, 667 (2008).
- [7] F. Schedin, A. K. Geim, S. V. Morozov, E. W. Hill, P. Blake, M. I. Katsnelson, K. S. Novoselov, *Nat. Mater.* **6**, 652 (2007).
- [8] A. K. Geim, *Science* **324**, 1530 (2009).
- [9] K. S. Kim, Y. Zhao, H. Jang, S. Y. Lee, J. M. Kim, J. H. Ahn, P. Kim, J. Y. Choi, B. H. Hong, *Nature* **457**, 706 (2009).
- [10] Y. M. Lin, C. Dimitrakopoulos, K. A. Jenkins, D. B. Farmer, H. Y. Chiu, A. Grill, P. Avouris, *Science* **327**, 662 (2010).
- [11] D. A. C. Brownson, D. K. Kampouris, C. E. Banks, *J. Power Sources* **196**, 4873 (2011).
- [12] C. Lee, X. D. Wei, J. W. Kysar, J. Hone, *Science* **321**, 385 (2008).
- [13] D. Braga, I. G. Lezama, H. Berger, A. F. Morpurgo, *Nano Lett.* **12**, 5218 (2012).
- [14] Z. Y. Yin, H. Li, L. Jiang, Y. M. Shi, Y. H. Sun, G. Lu, Q. Zhang, X. D. Chen, H. Zhang, *ACS Nano* **6**, 74 (2012).
- [15] Z. H. Dai, S. H. Liu, J. C. Bao, H. X. Jui, *Chem.-Eur. J.* **15**, 4321 (2009).
- [16] C. Wang, G. H. Du, K. Stahl, H. X. Huang, Y. J. Zhong, J. Z. Jiang, *J. Phys. Chem. C* **116**, 4000 (2012).
- [17] G. X. Wang, S. Bewlay, J. Yao, et al., *Electrochemical and solid-state letters* **7**, A321 (2004).
- [18] C. Feng, L. Huang, Z. Guo, et al., *Electrochem. Commun.* **9**, 119 (2007).
- [19] X. Fang, C. Hua, C. Wu, et al., *Chem.-Eur. J.* **19**, 5694 (2013).
- [20] R. Bhandavat, L. David, G. Singh, *The journal of physical chemistry letters* **3**, 1523 (2012).
- [21] H. Liu, D. Su, G. Wang, et al., *J. Mater. Chem.* **22**, 17437 (2012).
- [22] J. N. Coleman, L. Mustafa, O. Arlene, S. D. Bergin, P. J. King, U. Khan et al., *Science* **331**, 568 (2011).
- [23] H. S. S. Ramakrishna Matte, A. Gomathi, A. K. Manna, D. J. Late, R. Datta, S. K. Pati, et al., *Angew. Chem. Int. Ed.* **49**, 4059 (2010).
- [24] C. Altavilla, M. Sarno, P. Ciambelli, *Chem. Mater.* **23**, 3879 (2011).
- [25] X. Huang, Z. Y. Zeng, H. Zhang, *Chem. Soc. Rev.* **42**, 1934 (2013).
- [26] J. Yang, V. Damien, A. S. Joon, D. Kang, K. A. Young, C. Manish, et al., *Angew. Chem. Int. Ed.* **52**, 13751 (2013).
- [27] S. Ratha, C. S. Rout, *Acs Appl. Mater. Interfaces* **5**, 11427 (2013).
- [28] R. Tenne, L. Margulis, M. Genut, G. Hodes, *Nature* **360**, 444 (1993).